Equilibrium Theory Analysis of Vacuum Swing Adsorption for Separation of Ethanol from CO2 in Beverage Dealcoholisation Process

Equilibrium Theory Analysis of Vacuum Swing Adsorption for Separation of Ethanol from CO_2 in Beverage Dealcoholisation Process

Hyungwoong Ahn[1)*], Ju Hyun Lee[2)]

1) Institute for Materials and Processes, School of Engineering, The University of Edinburgh, Robert Stevenson Road, Edinburgh, EH9 3FB, UK

2) School of Engineering and Physical Sciences, Heriot-Watt University, Riccarton, Edinburgh, EH14 4AS, UK

*Corresponding author: H.Ahn@ed.ac.uk

Tel.: +44 131 650 5891

Abstract

In this study, a Vacuum Swing Adsorption (VSA) process was designed to recover ethanol from a binary gas mixture of ethanol and CO_2. The VSA feed gas originates in the process of alcoholic beverage dealcoholisation where ethanol is stripped off the standard beer by CO_2 flowing upward in the exchange column. The CO_2 recovery of the ethanol removal VSA has to be maintained as high as possible in order to improve the ethanol removal efficiency and reduce the energy consumption for both vacuum pump and ethanol trap. To this end, an ethanol recovery four-step VSA unit using MFI zeolites was analysed by Equilibrium Theory in which both non-linearity of ethanol isotherm and

incomplete purge were taken into account. The theoretical study revealed that the extent of purge had to be slightly greater than its minimum usage to achieve the maximum CO_2 recovery. In addition, the power consumption for evacuation and the process productivity per cycle were estimated. It turned out that, to minimise the specific power consumption, high desorption pressure and low extent of purge would be favoured. With a view to maximising the process productivity per cycle, the extent of purge has to be large. At the high extent of purge, the specific energy consumption can be saved by having the VSA run at low desorption pressure.

Keywords: Ethanol; zeolite; Equilibrium Theory; Vacuum Swing Adsorption; CO_2; Dealcoholisation; Non-linear isotherm; Incomplete purge

1. Introduction

Beers containing less alcohol has lately gained huge interests from the public due to burgeoning awareness of negative impact of alcohol consumption. With the demand growing, brewing technologies enabling to produce low alcohol beers are advancing accordingly [1, 2]. Selection of an appropriate dealcoholisation method is crucial as it does not affect simply capital and operating costs, but also the flavour of a low alcohol beer [3]. There are by large two cohorts of low alcohol beer production methods: physical methods that apply to standard beers from which ethanol is selectively removed by separation processes, and biological methods in which alcohol production is suppressed by a controlled/interrupted fermentation technology [4]. Physical methods are advantageous over biological methods in that they can control the alcohol contents more flexibly and also the beer products are by large of higher quality [5, 6]. However, extra capital investment and additional energy consumption are required to install and run the dealcoholisation process.

.

As for the separation technologies for dealcoholisation, distillation had been employed actively in the past but it involves huge energy consumption for heating and great loss of flavour-related aroma resulting from both thermal degradation of the compounds and non-selective removal of ethanol and aroma in the distillation column [4]. In practice, the conventional processes require auxiliary units for recovery of the aroma from ethanol by another distillation, followed by their blending with low-alcohol beers at the very end of the dealcoholisation process to recover the sensory quality[7]. But the original beer flavour is already compromised greatly in the thermal process. To tackle the issue, alternative physical dealcoholisation technologies have been developed that do not need to heat up the feed for ethanol removal.

Membrane-based technology is deemed as the best available technology for beer dealcoholisation and its commercial process has been widely used in industry[1]. Due to the low operating temperatures of membrane processes compared to thermal dealcoholisation methods, beer is not damaged by heat with its original taste and quality rarely affected [8]. Several studies have been reported for membrane-based dealcoholisation of other alcoholic beverages such as wine, apple cider and homemade beverage [9-12].

On the other hand, adsorptive dealcoholisation technologies are gaining good attention as a promising technology to compete with the membrane counterpart. Adsorptive dealcoholisation is worth investigation, as there are adsorbents readily available to remove ethanol selectively from water. It is well known that some hydrophobic porous materials, e.g. MFI zeolites, silicalite, activated carbons, etc., have a fairly large adsorption capacity of ethanol[13 14].

Accordingly, adsorptive dealcoholisation processes have been designed based on the hydrophobic zeolites [15, 16]. In 1983, Farhadpour et al. proposed an adsorptive process

to extract alcohol from beer using silicalite [17]. If follows that Anglerot invented an adsorptive process that removes ethanol from beer liquid. In the patent, the beer liquid is brought into direct contact with hydrophobic zeolites so that the beer ethanol can be removed from the beer. However, the aroma compounds that are crucial for beer flavour are also co-adsorbed by adsorbents and lost into the desorbate when the adsorbents are thermally regenerated. To tackle the issue, the desorbates are distilled to separate ethanol from aromas and the recovered aromas are blended with the raffinate to constitute a low-alcohol beer[2, 4]. As this invented technology must involve the distillation and blending steps in addition to the adsorptive dealcoholisation process, the capital cost is relatively high compared to the conventional method. In this respect, adsorptive ethanol removal technologies have to be developed and optimised yet to reduce the capital cost and energy consumption so significantly as to compete with membrane technologies for industrial applications [5].

Recently, Clariant put forward a new adsorption-based dealcoholisation process, claiming that it would be able to produce an alcohol-free beer from a standard beer more economically than the commercialised membrane process[18]. In the patented process, ethanol is removed from beers by flowing a gas, e.g. CO_2, through the beer and the ethanol-laden gas is processed in an adsorption process where ethanol is recovered from the gas mixture[18]. As most of the aroma compounds, e.g. isoamyl acetate, has a lower vapour pressure than ethanol, the amounts of aroma compound carried away by the gas in the stripping column must be less than that of ethanol. To the best of our knowledge, however, the ethanol removal adsorption process of the Clariant's system has not been studied theoretically in the open literature. In this study, a four-step Vacuum Swing Adsorption (VSA) system for selective ethanol removal from the gas mixture exemplified in the patent[18] is to be analysed using Equilibrium Theory and its optimal operating conditions are to be explored.

2. Process description of adsorptive beer dealcoholisation process[18]

The patented adsorptive dealcoholisation system is shown in Figure 1. In this process, a feed beer is pumped into an exchange column which it trickles down through contacting countercurrently a gas stream (CO_2 or N_2) flowing up the column. The exchange column is packed with Glass Raschig rings to increase the contact area between the gas and liquid phases. In the exchange column, ethanol must be the major component picked up by the gas as it is highly volatile compared to the others. Thus, there is no direct contact between the beer and adsorbent in case of the stripping-adsorption system. The arrangement of gas and liquid flows in the exchange column results in the required contact time between beer and gas streams being minimised, reducing flavour loss and preventing unnecessary foam formation. The beer stream leaving the exchange column contains substantially low ethanol in it and it is directly sent to a product tank. In this study, it was assumed that the ethanol contained in the beer would be stripped entirely off the beer by the CO_2.

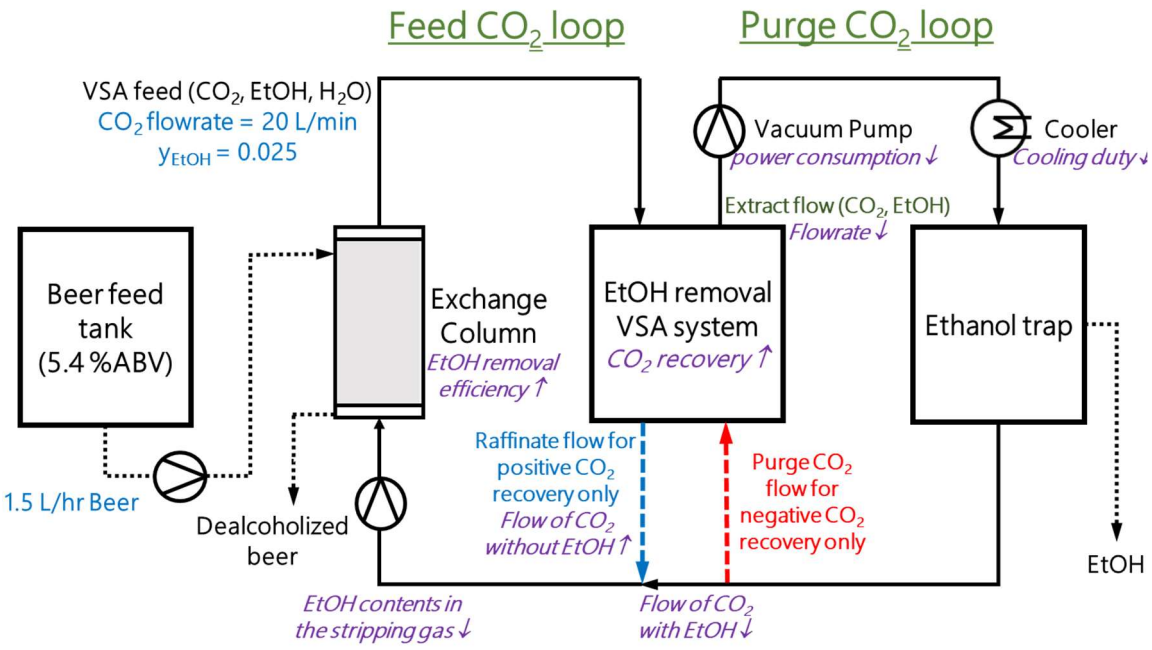

Figure 1. Process configuration of adsorptive dealcoholisation system and positive impacts effected by increasing VSA's CO_2 recovery.

The gas stream leaving the exchange column enters the adsorption column of a VSA system. According to the patent, an adsorbent made of MFI zeolite or silicalite is used to separate ethanol selectively from the gas mixture of ethanol, CO_2 and water vapour. Once the adsorbents are saturated with the heavy component, they have to be regenerated by desorbing the ethanol. The adsorption column is depressurised to a sub-atmospheric pressure and it follows that the column is purged by flowing CO_2 through the column at the reduced pressure. The gas stream leaving the column, containing CO_2 and ethanol, is cooled down at a heat exchanger in which the ethanol is condensed. The ethanol liquid is separated from CO_2 in the ethanol trap by phase separation. As ethanol is a highly volatile compound, it is hard to condense thoroughly the ethanol vapour even at sub-zero temperatures and the gas stream leaving the ethanol trap always contains some ethanol in it. In the stark contrast, the gas stream leaving the adsorption column of a VSA is practically ethanol-free due to strong adsorption of ethanol on the adsorbent. The stripping gas is comprised of the two gas streams originating from VSA and ethanol trap. Out of the two gases, the CO_2 gas from the VSA is favoured over the CO_2 gas from the ethanol trap. In the exchange column, the ethanol-free gas leaving the VSA can pick up more ethanol from the beer than the ethanol-laden gas flowing out of the ethanol trap.

The flowrate ratio of the two stripping gases is determined by CO_2 recovery of the VSA. The greater CO_2 recovery the VSA has, the more ethanol-free CO_2 gas is available for its use in the exchange column, resulting in the ethanol removal efficiency being improved in the exchange column. This indicates that the CO_2 gas flowrate of the purge CO_2 loop (see Figure 1) decreases with increasing CO_2 recovery, so that both vacuum pump and ethanol trap cooler can process less amount of gas. Accordingly, the energy consumption for two of them would be reduced. Therefore, it is crucial to have the ethanol removal VSA optimised in a way of maximising CO_2 recovery, in order to enhance the

ethanol removal efficiency and save the energy consumption at the same time.

3. Design of ethanol recovery VSA system by Equilibrium Theory model with non-linear isotherm and incomplete purge

An adsorptive dealcoholisation system was designed on the basis of the patented dealcoholisation technology[18]. A beer with 5.4 %ABV was used as a feed of the dealcoholisation system. The beer feed is processed at a rate of 1.5 L/h and CO_2 stream is supplied at 20 L/min as a stripping gas for the exchange column. Two different modes of operation were proposed by the inventors. In the semi-continuous mode, the beer stream leaving the exchange column is recycled back to the feed tank until the ethanol concentration reaches the low-alcohol beer target. In the present project, however, the beer is dealcoholised to whatever level is required after flowing the beer feed through the exchange column only once, i.e. once-through flow system, and the effluent from the exchange column is directed to a product tank without recycle as seen in Figure 1 (Continuous production).

Ethanol is removed by adsorption from the gas stream originating from the exchange column. The ethanol mole fraction of the gas mixture, y_F = 0.025, was estimated from the gas and liquid flowrates around the exchange column (see Figure 1) based on the ethanol vapour pressure given the temperature. For simplicity's sake, it was assumed that the feed gas entering the adsorption column would be a binary mixture of ethanol and CO_2 carrier gas, with the other trace components and water vapour lumped into CO_2.

The first step of the adsorption process is to select the appropriate hydrophobic adsorbent suitable for selective removal of ethanol from CO_2. Past research papers were reviewed to evaluate various adsorbents with respect to the ethanol selectivity and

adsorption amounts [14, 19, 20]. Zhang et al. investigated adsorption equilibrium of ethanol vapour on MFI type zeolite [14]. In their study, the experimental data were fitted well by Sircar's model, which is expressed by:

$$\frac{q}{q_s} = \frac{C1\left(\frac{P}{P0}\right)\left[1+(C2-1)\left(\frac{P}{P0}\right)\right]}{\left(1-\frac{P}{P0}\right)\left[1+(C1-1)\left(\frac{P}{P0}\right)\right]} \quad (1)$$

where C1 and C2 are temperature-dependent constants describing the adsorbate-adsorbent interactions in the first layer and in the subsequent layers, respectively [21]. q is adsorption amount, q_s is saturation limit of adsorption amount, p is pressure and p_0 is saturated vapour pressure [14].

In this adsorption system, CO_2 is a weakly adsorbing component. Vidoni et al. measured adsorption amounts of CO_2 on silicalite and Langmuir model was used to fit the CO_2 adsorption isotherms [22]. The model is expressed by:

$$\frac{q}{qs} = \frac{bp}{1+bp} \quad (2)$$

where $b \cdot q_s$ is the slope of the isotherm when pressure approaches zero [23] and the linear isotherm was taken for Equilibrium Theory analysis in this study. The two equilibrium isotherm models were taken to estimate the adsorption amounts of ethanol and CO_2 per unit mass of adsorbent. The ethanol and CO_2 isotherms were plotted at different temperatures in Figure 2. All the isotherm parameters are listed in Table 1.

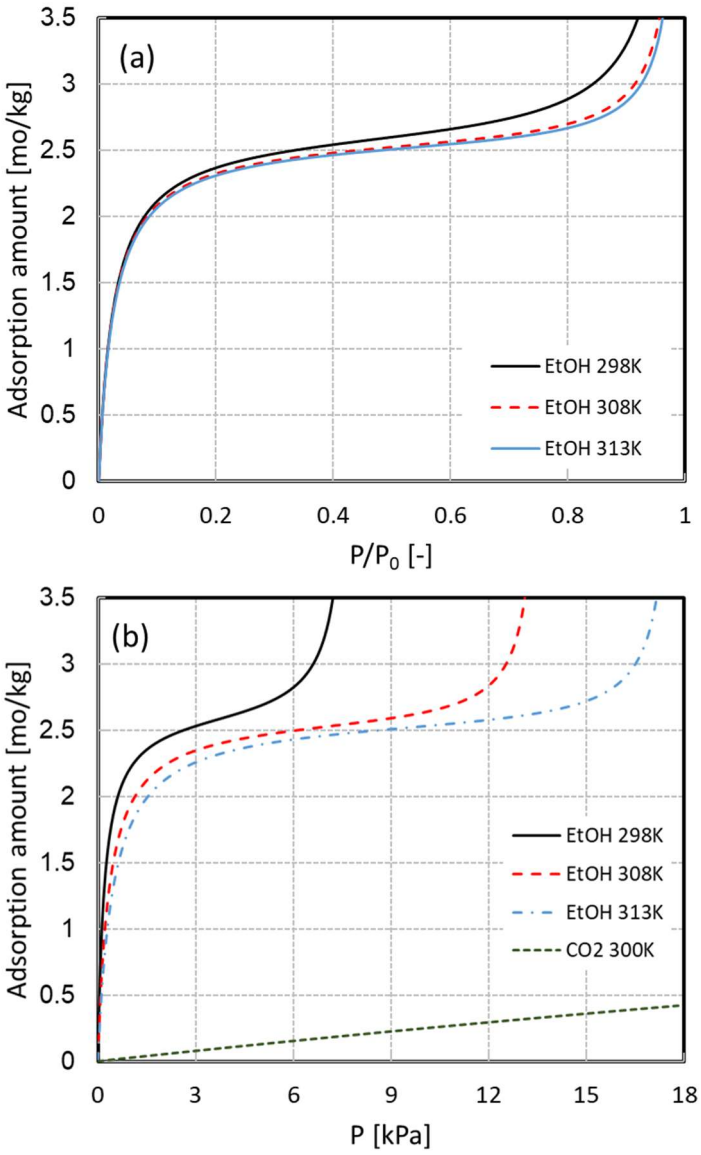

Figure 2. Adsorption isotherm of ethanol and CO_2 for MFI type zeolites [14, 22]

The adsorption equilibrium isotherms of ethanol vapour are categorised into Type IV isotherm by IUPAC classification, indicating capillary condensation takes place at high pressures approaching the saturation pressure [24]. As seen in Figure 2, the ethanol isotherms deviate so greatly from linearity that they cannot be approximated by linear isotherms, while the CO_2 isotherm is closer to linearity. Given the shapes of isotherms, it is clear that the heavy component's adsorption equilibrium must be predicted by an

isotherm model that is not linear, such as Eq.1, while the light component isotherm can be simplified into a linear isotherm of which the slope is $b \cdot q_s$ of the Langmuir isotherm.

To enable continuous operation of adsorptive separation, an adsorption process must consist of more than two columns, so that a column is regenerated for its use in the next cycle while another column processes the feed for ethanol removal. A variety of new cyclic adsorption processes have been proposed since a Pressure Swing Adsorption (PSA) was firstly invented by Skarstrom in 1960[25]. While the process performances are affected by both adsorption equilibrium and kinetics, analysis of an adsorption process can be simplified greatly by Equilibrium Theory in which adsorption kinetic effects are neglected [26]. Equilibrium Theory has since been developed further to analyse various adsorption systems, e.g. a PSA system with linear isotherm[27, 28], a PSA system with nonlinear isotherms[29, 30], effect of incomplete purge in a PSA system[31], adiabatic temperature swing adsorption system[32], etc.

In this study, a simple four-step, two-column VSA cycle is taken for ethanol removal from the gas mixture. As shown in Figure 3, the VSA cycle is comprised of four steps: Feed, Blowdown, Purge and Light component pressurization [26]. Dimensions and parameters of adsorption column are listed in Table 1.

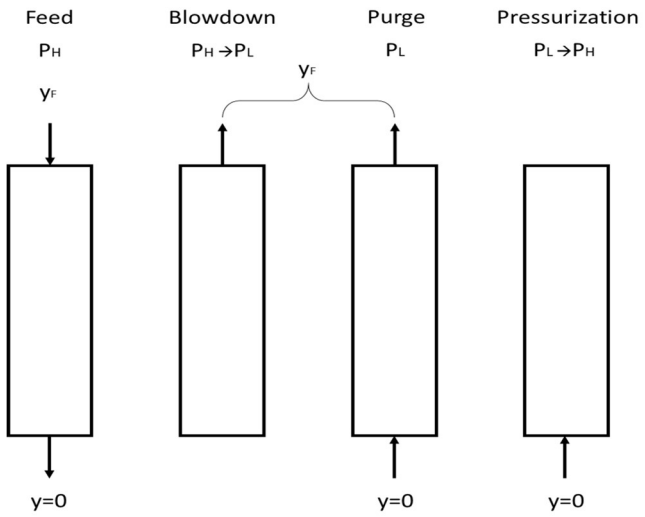

Figure 3. Graphical depiction of gas flow direction and pressure change at each step of four-step ethanol removal VSA

Table 1. Parameters for adsorption column and isotherm models of the ethanol removal VSA system.

Adsorption Column Parameters	
PSA feed flowrate, Q_F [m^3/s]	$3.11\ 10^{-4}$
Ethanol mole fraction in the PSA feed, y_F [-]	0.025
Interparticle void fraction, Ɛ [-]	0.5
Adsorption pellet density, ρ_s [kg/m^3]	900
Column length, L [m]	1
Column diameter, D [m]	0.023
Column cross sectional area, A [m^2]	$4.16\ 10^{-4}$
Temperature [K]	298
Sircar's Isotherm parameters for ethanol adsorption on MFI zeolites at 298K [21]	
q_s [mol/kg]	2.55
C1	40
C2	0.031
Langmuir Isotherm parameters for CO_2 adsorption on MFI zeolites at 298K [23]	
b [Pa^{-1}]	$0.75\ 10^{-5}$
q_s [mol/kg]	3.5

The following assumptions that generally apply to Equilibrium Theory are valid for this study too.

- The feed is a binary mixture of light component, CO_2, and heavy component, ethanol.
- The light component isotherm is approximated by a linear isotherm, while the heavy component isotherm is non-linear. The two isotherms are not coupled.
- Isothermal operation.
- Negligible pressure drop along the column, i.e. no pressure drop.

- Instantaneous equilibrium between gas and adsorbed phases, no mass transfer resistances.
- Plug flow with negligible axial dispersion.
- The purge gas is a pure CO_2, though in reality the CO2 gas originating from ethanol trap is likely to contain some ethanol in it.

Based on these assumptions, Kayser and Knaebel developed the Equilibrium Theory model of a 4-step PSA where the heavy component's isotherm is nonlinear, to estimate the light component recovery and the heavy component purity in the extract[30]. But the model is highly limited to a case where the column is completely regenerated during the purge step. The assumption of complete regeneration seems not realistic, as a column is seldom fully regenerated in the actual operation. This is the case in particular when the isotherm is so highly nonlinear that the amount of purge gas required for complete regeneration is gigantic. Therefore, it is essential to use a mathematical model capable of estimating the performance with both incomplete purge and nonlinear isotherm taken into account.

At the end of adsorption step, the adsorption column is completely saturated with the feed at 120 kPa and 298 K, and ethanol is present at its mole fraction in the feed, y_F, over the entire column. At this condition, the number of moles of each component that remains in the column is estimated by:

$$W_{F,A} = \frac{P_H y_F \varepsilon AL}{RT\theta_A},\ W_{F,B} = \frac{P_H (1-y_F)\varepsilon AL}{RT_B} \quad (3)$$

During the subsequent blowdown step, the heavy component's mole fraction gets increased as the strongly adsorbed component desorbs more than the light component. Again the gas mole fraction is constant spatially throughout the column, while it changes with decreasing pressure. The gas mole fraction varying with pressure can be estimated

by:

$$dy = \frac{y(y-1)(1-\beta)}{1+(\beta-1)y} dlnP \quad (4)$$

where the slope of the nonlinear heavy component isotherm does change greatly with pressure. As the slope of isotherm is not constant and neither is β, this equation has to be solved numerically. Eq.4 is rearranged and integrated as follows:

$$\int_{y_1}^{y_2} \frac{1}{(\beta-1)y} + \frac{\beta}{(1-\beta)(y-1)} dy = \int_{P_1}^{P_2} \frac{1}{P} dP \quad (5)$$

The LHS can be integrated easily if β is a function of y only, in other words, it is independent of pressure. To this end, the entire integration range of the RHS, P_H to P_L, is divided into so many sub-sections that β can be practically independent of pressure over the tiny integration range of the individual integrations. It is important to check if the number of sections dividing the entire integration range is large enough to ensure that the result of integration would not be affected by selection of the section numbers.

The ethanol mole fraction was estimated at a pressure to which the column is depressurised from the adsorption pressure. The ethanol mole fraction in the column gets increased up to 0.46 from 0.025 with the column pressure reduced to 3 kPa from 120 kPa as shown in Figure 4.

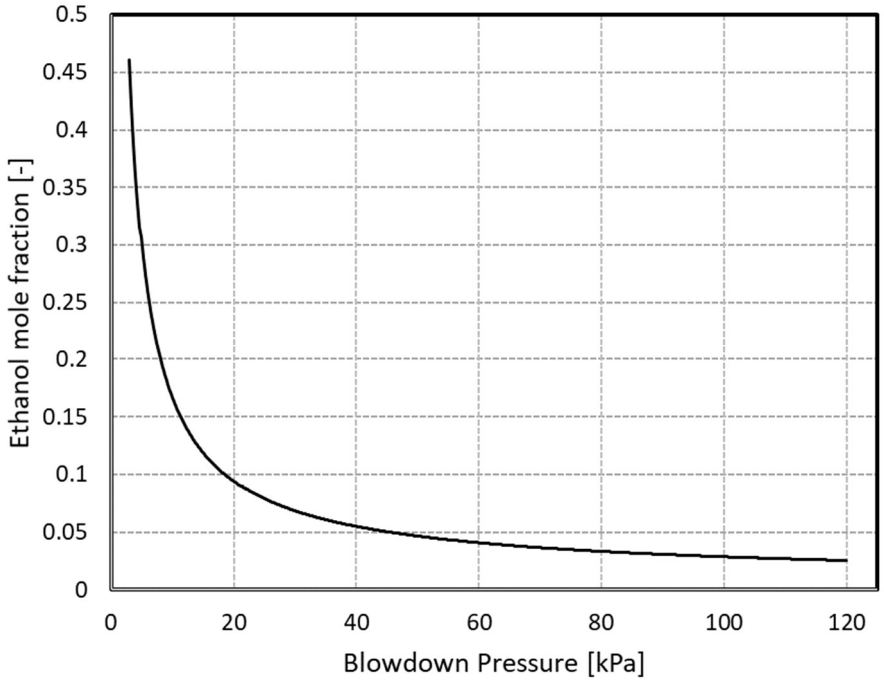

Figure 4. Ethanol mole fraction in the gas phase at the end of blowdown step: Effect of blowdown pressure.

In the purge step, the column is regenerated by flowing pure CO_2 through the column in the direction opposite to the feed flow (Figure 3). Reducing the partial pressure of ethanol in the gas phase facilitates desorbing ethanol off adsorbents. Once desorbed, ethanol travels toward the column outlet along with the purge flow and it is expelled out of the column when it reaches the end of the column. The extent of column regeneration is affected greatly by the amount of purge gas consumed in the purge step. The greater the purge gas consumption becomes, the more thoroughly does a column get regenerated. The column containing less heavy component is able to process more feed in the next adsorption step, resulting in greater bed productivity per cycle. On the contrary the energy consumption per cycle for evacuation gets larger with the purge gas consumption increasing. However, the specific power consumption may not show such a trend of increasing monotonously with the purge gas consumption as the simple power

consumption per cycle does. Given the relatively small slope of isotherm at high pressures, the adsorption column can be regenerated so efficiently in the initial phase of purge. But the efficiency of column regeneration gets worse quickly with the slope of isotherm large at low pressures where ethanol is very hard to desorb. In this respect, consumption of the purge flow needs to be optimised for maximising CO_2 recovery or reducing the specific energy consumption with good throughput achieved. However, the optimum purge gas amount must be searched between the upper and lower limits of the purge gas consumption that are defined below.

The lower limit of purge gas consumption is found by estimating the purge gas amount that is required to push the ethanol profile to an extent that the ethanol plateau at the highest mole fraction reaches the outlet. At the end pressure of blowdown step of 12 kPa, the ethanol mole fraction in the column, y_b, was estimated 0.143 in this study. Given the shape of the ethanol isotherm in Figure 2, the ethanol front must be a simple wave in which the high concentration plateau propagates faster along the column than the low concentration plateau during desorption. Accordingly, the ethanol plateau at the highest mole fraction, y_b, travels fastest and reaches the column end first during the purge step. If the purge gas amount was less than the minimum, the ethanol mole fraction around the column near the outlet is still y_b. When it is pressurised back to the adsorption pressure in the next cycle, the ethanol mole fraction of y_b returns to y_f, i.e. 0.025. This means that the section of the bed where the ethanol mole fraction is still y_b at the end of purge step would have no capacity to adsorb ethanol in the next feed step. Therefore, it is important to see how fast the ethanol plateau at y_b moves along the column during the purge step. The ethanol front velocity at y_b is estimated by:

$$\left(\frac{dz}{dt}\right)_{y_b} = \frac{\beta_A u_{PG}}{[1+(\beta-1)y_b]^2} \tag{6}$$

The extent of purge, X, is defined as the ratio of the distance of clean section

containing no heavy component to the entire column length[28, 31]. The minimum extent of purge, X_{min}, corresponds to the minimum purge gas amount defined above and it is estimated by:

$$X_{min} = \frac{\beta_{A0} u_{PG} t_{min}}{L} = \frac{\beta_{A0} u_{PG}}{\left(\frac{dz}{dt}\right)_{y_b}} \quad (7)$$

where t_{min} is the time required for the ethanol plateau at y_b to reach the column end.

On the other hand, the upper limits of purge gas amount is defined as the purge gas amount required to regenerate the column completely, i.e. X=1. The number of moles of the purge gas required for X=1 is estimated as $\Phi = \frac{P_L \varepsilon A L}{RT}_{A0} = \frac{P_L \varepsilon A}{RT}_{PG} t_{max}$.

The actual purge gas amount must lie between the two limits and it is calculated by:

$$N_{PG} = \frac{\varepsilon u_{PG} A P_L t_{PG}}{RT}, \qquad t_{min} \leq t_{PG} \leq t_{max} \quad (8)$$

In this study, purge step time, t_{PG}, was varied in the range of 1 to 20 times t_{min} to see the effect of the purge gas amount on the ethanol mole fraction profile at the end of the purge step. The ethanol mole fraction profiles were plotted in Figure 5 at varying purge gas consumption, i.e. varying extents of purge, X.

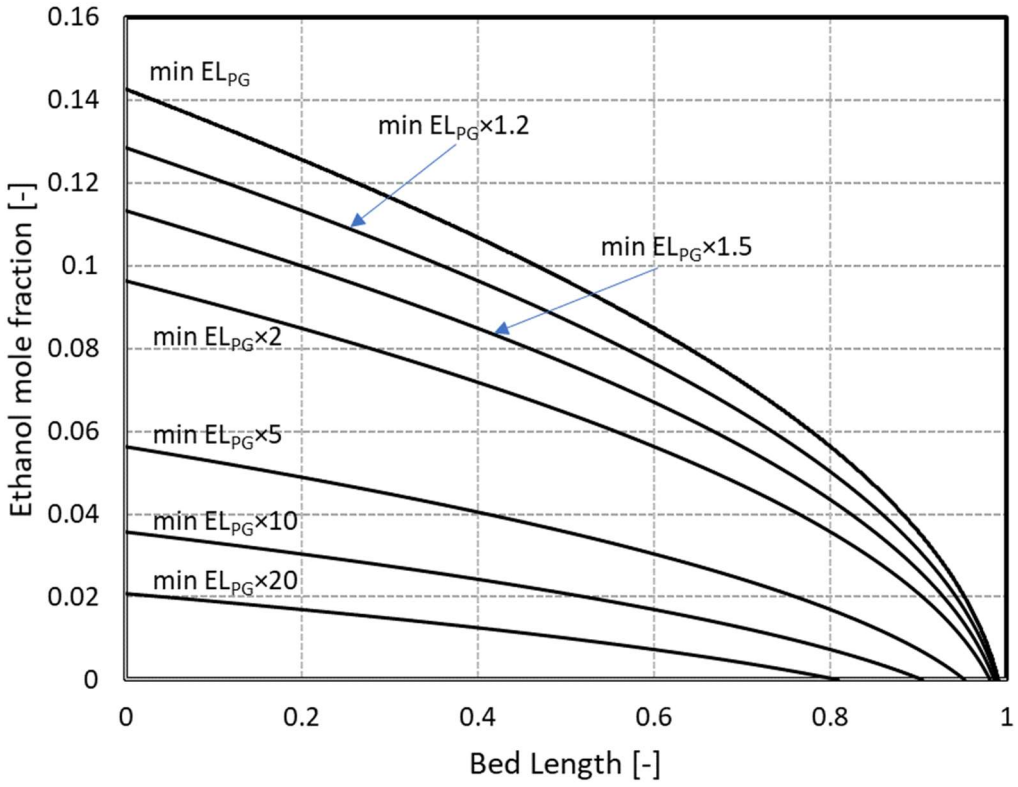

Figure 5. Ethanol mole fraction profile at the end of purge step: Effect of purge gas amount.

As can be seen in Figure 5, the ethanol profile was pushed further to the left with increasing purge gas amount. Note that the fraction of the column section containing no ethanol over the column length, X, is rather small in this case, which is attributed to the extremely high nonlinearity of ethanol isotherm (Figure 2). Only 20% increase of the purge gas amount from the minimum use, 1.2 t_{min} case in Figure 5, makes a noticeable impact on the ethanol profile. But the positive effect incurred by increasing purge gas amount gets diminished fast with increasing purge gas amount, so the effect incurred by the first 20% increase to 1.2 t_{min} is almost comparable to the difference made by increasing from 10 t_{min} to 20 t_{min}, with respect to the ethanol mole fraction at the column outlet. This is because the slope of isotherm increases with decreasing ethanol partial pressure, in order words, the ethanol at a low concentration close to zero is hard to

desorb and its plateau propagates so slow. This implies that the purge gas amount has to increase substantially to see any noticeable difference in the ethanol profile in the region of low ethanol partial pressure.

In the following CO_2 pressurisation, the column is pressurised back to the adsorption pressure with a CO_2 stream flowing through the column end which it is admitted to during the purge step. Accordingly, the amount of ethanol present in the column remains unchanged and is the same as that at the end of the purge step that precedes the pressurisation step. While we are not interested in how ethanol is distributed exactly along the column, it is crucial to estimate the location of zero ethanol plateau for analysis of the adsorption step that follows the CO_2 pressurisation step. The location of zero ethanol plateau, z_f, is estimated by solving the following integration.

$$\int_{1-X}^{z_f} \frac{1}{z} dz + \frac{1}{\beta_B} \int_{P_L}^{P_H} \frac{\beta_{A0}}{P} dP = 0 \quad (9)$$

As a result of CO_2 pressurisation, the location of zero ethanol plateau is slightly pushed toward the feed end. Whereas the moles of ethanol present in the column must remain unchanged around the step, the moles of CO_2 in the column increase by the amount of CO_2 injected into the column for pressurisation. The moles of CO_2 entering the column during pressurisation are:

$$N_{Pr,L} = \Phi \beta_0 \left(\frac{P_H}{P_L} - 1 \right) \quad (10)$$

Given the shape of the isotherm, a shock front is to be formed along the column during the feed step, but the shock front has an ethanol mole fraction range of which the lower end is changing, until it is fully developed from 0 to y_f. Due to the heavy component existing in the column at the start of feed step (incomplete purge), the lower bound of the shock front is not zero initially but it decreases gradually to zero as the shock front evolves. Once a perfect shock front is formed, its propagation velocity can be estimated by the weak solution of the mass balance differential equation. It is possible to estimate

the location where the fully developed shock forms first, Y_s, and the time required to see the lower bound of the shock front reach zero, t_s. The following two independent equations are established to find Y_s and t_s, given the fact that both shock front and zero ethanol plateau must reach Y_s at t_s[28].

$$\beta_{A0} u_F [1 + (\beta - 1) y_F] t_S - Y_S = -z_f \tag{11a}$$

where β is assumed constant in the narrow range of y.

$$\frac{\varepsilon A u_F P_H y_F}{RT} t_S - \frac{\varepsilon A P_H y_F}{RT \theta_A} Y_S = -\frac{\sum_i \Phi \beta_{A0} y_{PG,i} \left[1 + \frac{1-\varepsilon}{\varepsilon} \frac{\Delta q_i}{\Delta p_i} \rho_p RT\right] \Delta z_i}{\sum_i \Delta z_i} \tag{11b}$$

Once the shock front is fully developed, it travels from Y_s to the column end at the speed of $\theta_A v_F$.

For each of four steps, the moles of gas entering and leaving the column were estimated for each component, by simply using the mass balance around the column. Subsequently, the light component product recovery and the heavy component purity in the extract were calculated.

As for the four-step VSA of this study using Equilibrium Theory, the CO_2 recovery is of great importance while the ethanol recovery is always 100%. The light component product recovery is widely used as the performance indicator of a cyclic adsorption process [33-36]. The CO_2 recovery of a VSA process, R_B, is estimated as below [30]:

$$R_B = \frac{N_{FP} - N_{PR} - N_{PG}}{N_F (1 - y_F)} \tag{12}$$

where N_{FP} is the moles of CO_2 that leave the column during feed step, N_{PR} is the moles of CO_2 consumed for pressurization, N_{PG} is the moles of CO_2 consumed for regeneration during purge step, and N_F is the moles of the VSA feed entering the column during feed step.

4. Parametric study

A cyclic adsorption process can be optimised differently depending on the way of formulating the objective function factoring in product purity/recovery, bed productivity and energy consumption. In optimising the ethanol recovery VSA of this study, the CO_2 recovery is of the greatest importance of all, as it has great impact on performance of the dealcoholisation process, such as ethanol removal efficiency at the exchange column and energy consumptions at the vacuum pump and ethanol trap. . In this study, the CO_2 recovery of the ethanol VSA was investigated by varying the two important operating parameters: one is the extent of purge and the other is the desorption pressure.

4.1. Effect of extent of purge

It is well known that the extent of purge is a parameter that has a direct impact on the light component recovery. According to Eq. 12, all the variables but moles for pressurisation, N_{PR}, are highly affected by the extent of purge. In case of linear isotherms being taken for both heavy and light components, the light component recovery decreases monotonously with increasing extent of purge[26, 37]. It is interesting to see the effect of the extent of purge on the CO_2 recovery in this adsorption system where the heavy component isotherm is highly non-linear. The CO_2 recovery was calculated using the model described above at varying extents of purge ranging from the minimum to one. The results are presented under three desorption pressures: 3, 12 and 48 kPa that are equated to 0.025, 0.1 and 0.4 in terms of pressure ratio, P_R, in Figure 6.

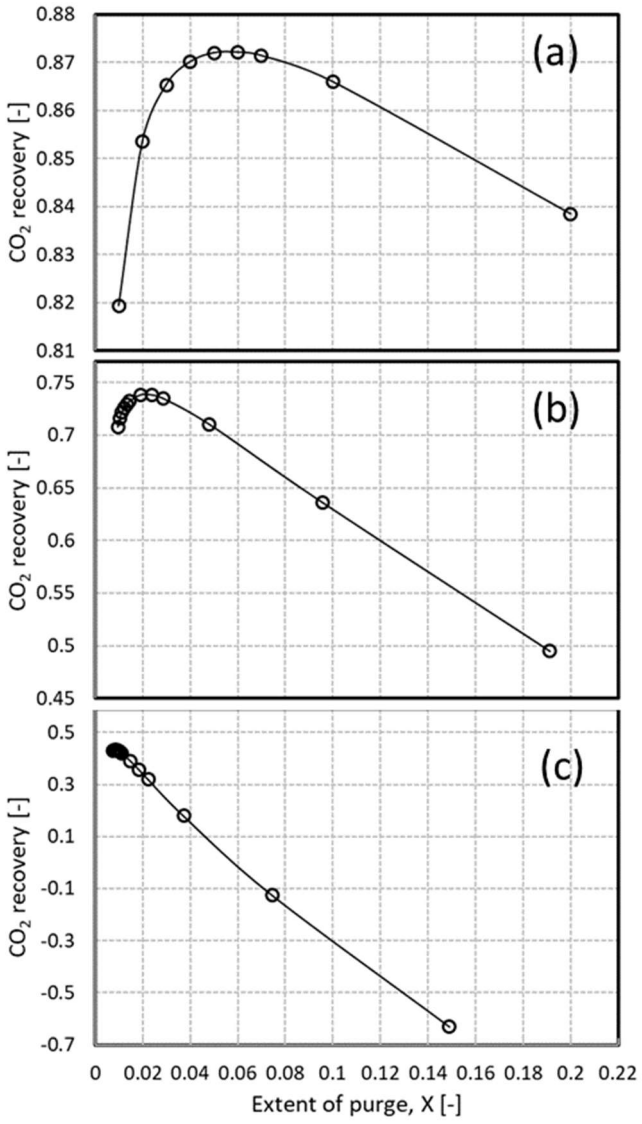

Figure 6. Effect of the extent of purge on CO_2 recovery at three different desorption pressures: (a) 3 kPa, (b) 12 kPa and (c) 48 kPa.

At 3 kPa of desorption pressure (P_R = 0.025), it was observed that the CO_2 recovery reached the maximum of 87.21% around X = 0.060. This can be explained by non-linearity of the highly favourable ethanol isotherm (Figure 2). Increasing the purge gas consumption in the range of X from the minimum to 0.06 is so efficient in regenerating the column that the gain of CO_2 recovery resulting from processing more feed is greater than the loss of CO_2 recovery caused by spending more purge gas. It is noticeable that the X value resulting in the maximum recovery decreases with increasing desorption

pressure, that is, the optimal X value changes to 0.019 from 0.06 when the desorption pressure increases to 12 kPa from 3 kPa. At the desorption pressure of 48 kPa, the optimal X value is very close to the minimum extent of purge, i.e. X = 0.0082 at 48 kPa.

The extent of purge also has a significant effect on the productivity and specific energy consumption. As shown in Figure 7, the amount of ethanol produced per one cycle increases greatly with the extent of purge, as the more rigorously a column is regenerated, the greater feed it can process during the feed step.

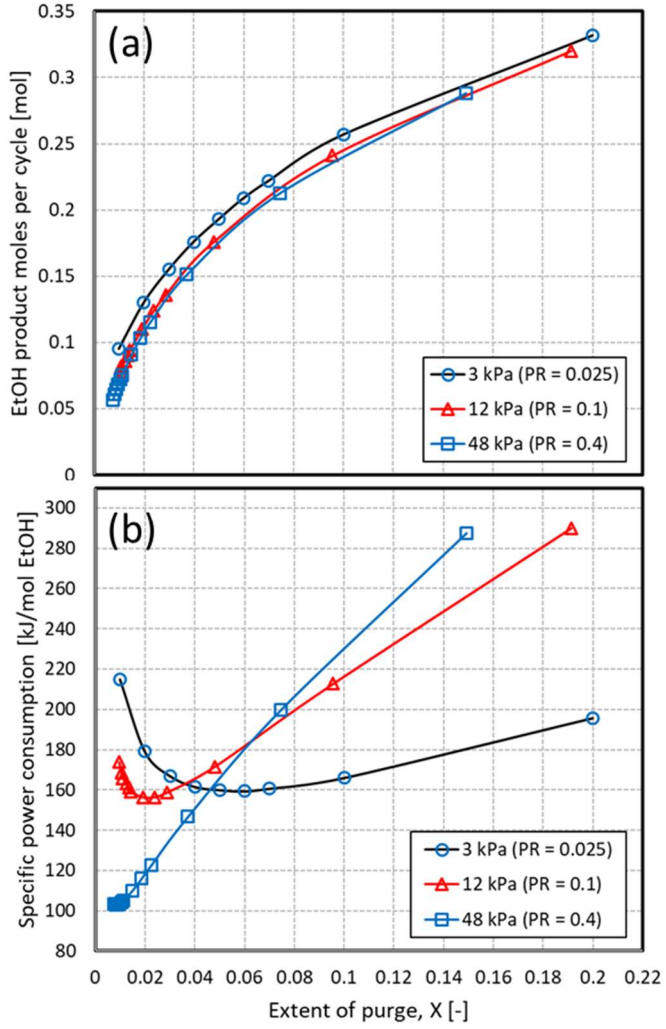

Figure 7. Effect of the extent of purge on (a) the productivity of a cycle and (b) specific power consumption of vacuum pump at three different desorption pressures (pressure ratio).

The power consumption of a vacuum pump for column evacuation accounts for majority of the VSA energy consumption. As shown in Figure 7b, the VSA running at the high desorption pressure (48 kPa) spends least power in the range of X from the minimum to 0.05. But in the range of X greater than 0.05, the VSA running at the lowest desorption pressure (3 kPa) becomes most advantageous in terms of specific power consumption. In comparing two figures of Figure 7, it can be seen that the power consumption would become by large greater when a high productivity is needed,

regardless of the desorption pressure. Therefore a trade-off between the process productivity per cycle and the specific energy consumption was observed. In other words, the column size has to be larger to reduce the energy consumption or vice versa.

4.2. Effect of pressure ratio

The effect of the pressure ratio on the CO_2 recovery was evaluated at three different extents of purge: X = 0.01, 0.1 and 1 (complete regeneration) and the results are presented in Figure 8. All three plots show a monotonous decrease with increasing pressure ratio, indicating that it would be hard to achieve high CO_2 recovery in case of the desorption pressure not being so low. As shown in Figure 8, the lower the extent of purge (X) is, the higher CO_2 recovery is achievable. But this is not true for the cases of the pressure ratio (P_R) being less than 0.1. It shows that the X = 0.1 case has a greater CO_2 recovery than the X = 0.01 case in the range of the pressure ratio being less than 0.05. These results are consistent with what were observed in Figure 6a where the effect of extent of purge on CO_2 recovery was shown at the desorption pressure of 3 kPa. At the lowest pressure ratio (P_R=0.025), the optimal extent of purge was around 0.06, and the CO_2 recovery at X=0.1 was greater than that at X = 0.01.

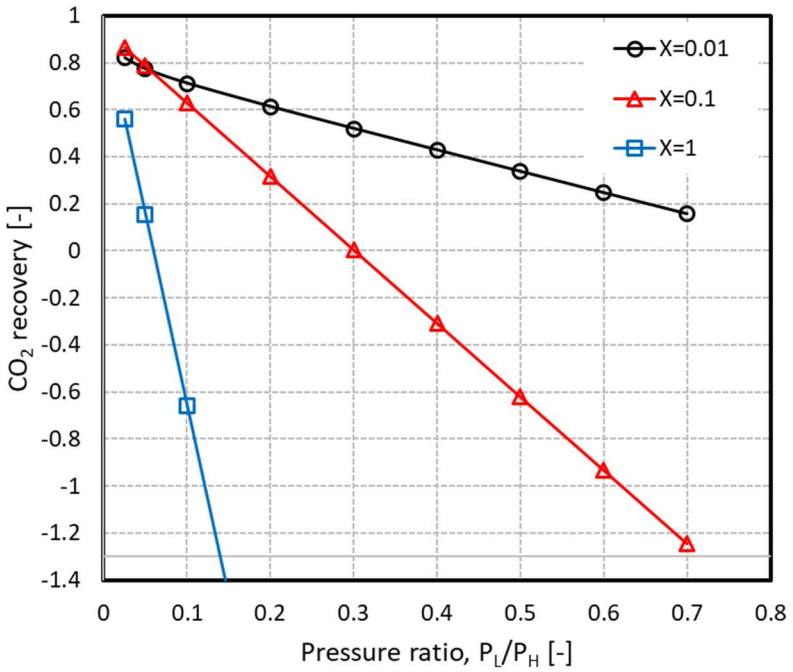

Figure 8. Effect of the pressure ratio (or desorption pressure) on CO_2 recovery at three different extents of purge.

5. Conclusions

For adsorptive beer dealcoholisation, a hydrophobic MFI type zeolites are often taken for selective removal of ethanol from CO_2. The adsorption isotherm of ethanol on the zeolite is so favourable that the non-linearity of the isotherm must be considered for analysis of the process. A four-step Vacuum Swing Adsorption (VSA) process was analysed by Equilibrium Theory model with non-linear heavy component isotherm and incomplete purge. As a result, it was discovered that:

- At a fixed desorption pressure, the maximum CO_2 recovery is achievable around an extent of purge that is slightly greater than the minimum extent of purge. Note that the extent of purge for the maximum recovery varies with the desorption pressure (pressure ratio) and it converges to the minimum purge with increasing desorption pressure.

- The four-step VSA system for ethanol recovery can be optimised differently for a selected performance index that is considered the most important of all. To minimise the specific power consumption, for example, it is recommended to operate the VSA at a relatively high desorption pressure with the extent of purge kept low.
- If the process productivity per cycle needs to be large to reduce the column size, the VSA must be operated at high extents of purge. With the extent of purge fixed at a high value, the specific power consumption can be minimisedby decreasing the desorption pressure.

Nomenclature

A	Column cross-sectional area (m^2)
b	Langmuir isotherm parameter, Eq. 2 (1/kPa)
$C1$ $C2$	Temperature-dependent constants of Sircar's isotherm model, Eq. 1 (-)
EL_{PG}	Total number of moles of purge gas used during purge step
L	Column length (m)
N_{PG}	Moles of purge gas consumed during the purge step (mol)
P	Pressure (kPa)
P_H	Adsorption pressure (kPa)
P_L	Desorption pressure (kPa)
P_0	Saturation pressure (kPa)
R_B	Recovery of the light component (-)
q	Adsorbed amount at equilibrium (mol/kg)
q_s	Saturated adsorption amount (mol/kg)
R	Universal gas constant (kPa·m^3/mol/K)
T	Temperature (K)
t_S	Time taken for a shock front to be fully developed (s)
u	Interstitial gas velocity (m/s)
W	Moles of gas existing in the column (mol)
y	Gas mole fraction (-)
y_b	Ethanol mole fraction in the gas phase at the end of blowdown step (-)
y_F	Ethanol mole fraction in the feed gas (-)
Y_S	Location of a shock front when it is fully developed (m)
z_f	Location of zero ethanol plateau (m)

Greek Letters

β	β_A / β_B (-)

β_i	$\frac{1}{1+\frac{1-\varepsilon}{\varepsilon}\left(\frac{dq_i}{dp_i}\right)\rho_p RT}$ (-)
θ	$\theta_A / \theta_B = \theta_A / \beta_B$ (-)
θ_i	$\frac{1}{1+\frac{1-\varepsilon}{\varepsilon}\left(\frac{\Delta q_i}{\Delta p_i}\right)\rho_p RT}$ (-)
ε	Interparticle void fraction in the bed (-)
Φ	Moles of purge gas required for complete purge (mol)
ρ_p	Adsorbent density (kg/m^3)

Subscripts

0	Zero pressure
A	Heavy component, ethanol
B	Light component, CO_2
F	Feed step
FP	Product stream leaving the column during feed step
PG	Purge step
PR	Pressurisation

References

1. Güzel, N.; Güzel, M.; Savaş Bahçeci, K., Chapter 6 - Nonalcoholic Beer. In *Trends in Non-alcoholic Beverages*, Galanakis, C. M., Ed. Academic Press: 2020; pp 167-200.
2. Anglerot, D. Process of making alcohol-free beer and beer aroma concentrates. US Patent 5308,631, 1994.
3. Müller, M.; Bellut, K.; Tippmann, J.; Becker, T., Physical Methods for Dealcoholization of Beverage Matrices and their Impact on Quality Attributes. *ChemBioEng Reviews* **2017,** 4, (5), 310-326.
4. Brányik, T.; Silva, D. P.; Baszczyňski, M.; Lehnert, R.; Almeida E Silva, J. B., A review of methods of low alcohol and alcohol-free beer production. *Journal of Food Engineering* **2012,** 108, (4), 493-506.
5. Sohrabvandi, S.; Mousavi, S. M.; Razavi, S. H.; Mortazavian, A. M.; Rezaei, K., Alcohol-free Beer: Methods of Production, Sensorial Defects, and Healthful Effects. *Food Reviews International* **2010,** 26, (4), 335-352.
6. Muller, C. N., L.E.; Gomes, L.; Guimaraes, M.; Ghesti, G., Processes for Alcohol-free Beer Production: a Review. *Food Science and Technology* **2019,** 40, (2), 273 - 281.
7. Liguori, L.; De Francesco, G.; Russo, P.; Perretti, G.; Albanese, D.; Di Matteo, M., Production and characterization of alcohol-free beer by membrane process. *Food and Bioproducts Processing* **2015,** 94, 158-168.
8. Catarino, M.; Mendes, A.; Madeira, L. M.; Ferreira, A., Alcohol Removal From Beer by Reverse Osmosis. *Separation Science and Technology* **2007,** 42, (13), 3011-3027.
9. Gil, M.; Estévez, S.; Kontoudakis, N.; Fort, F.; Canals, J. M.; Zamora, F., Influence of partial dealcoholization by reverse osmosis on red wine composition and sensory characteristics. *European Food Research and Technology* **2013,** 237, (4), 481-488.
10. López, M.; Alvarez, S.; Riera, F. A.; Alvarez, R., Production of Low Alcohol Content Apple Cider by Reverse Osmosis. *Industrial & Engineering Chemistry Research* **2002,** 41, (25), 6600-6606.
11. Pilipovik, M.; Riverol, C., Assessing dealcoholization systems based on reverse osmosis. *Journal Of Food Engineering* **2005,** 69, (4), 437-441.
12. Catarino, M.; Mendes, A., Dealcoholizing wine by membrane separation processes. *Innovative Food Science and Emerging Technologies* **2011,** 12, (3), 330-337.
13. Cartón, A.; Benito, G. G.; Rey, J. A.; de la Fuente, M., Selection of adsorbents to be used in an ethanol fermentation process. Adsorption isotherms and kinetics. *Bioresource Technology* **1998,** 66, (1), 75-78.
14. Zhang, K.; Lively, R. P.; Noel, J. D.; Dose, M. E.; McCool, B. A.; Chance, R. R.; Koros, W. J., Adsorption of Water and Ethanol in MFI-Type Zeolites. *Langmuir* **2012,** 28, (23), 8664-8673.
15. Abdehagh, N. D., B; Thibault, J.; Tezel, F.H., Biobutanol Separation from ABE Model

Solutions and Fermentation Broths Using a Combined Adsorption - Gas Stripping Process. *Journal of Chemical Technology and Biotechnology* **2017,** 92, 245 - 251.

16. Kim, B.; Jang, H.; Eom, M.-H.; Lee, J. H., Model-based Optimization of Cyclic Operation of Acetone-Butanol-Ethanol (ABE) Fermentation Process with ex Situ Butanol Recovery (ESBR) for Continuous Biobutanol Production *Industrial & Engineering Chemistry Research* **2017,** 56, 2071 - 2082.

17. Farhadpour, F. A.; Bono, A.; Tuzun, U., Separation of alcohol-water mixtures by liquid phase adsorption. In *European Symposium on Biotechnology*, Nutfield, GB, 1983.

18. Bertsch, S.; Verhuelsdonk, M.; Zavrel, M.; Gensler, S. Method for Dealcoholization of Beverages. Patent WO/2019/243144, 2019.

19. Hashi, M.; Tezel, F. H.; Thibault, J., Ethanol Recovery from Fermentation Broth via Carbon Dioxide Stripping and Adsorption. *Energy & Fuels* **2010,** 24, (9), 4628-4637.

20. Kuhn, J.; Castillo-Sanchez, J. M.; Gascon, J.; Calero, S.; Dubbeldam, D.; Vlugt, T. J. H.; Kapteijn, F.; Gross, J., Adsorption and Diffusion of Water, Methanol, and Ethanol in All-Silica DD3R: Experiments and Simulation. *The Journal of Physical Chemistry C* **2009,** 113, (32), 14290-14301.

21. Sircar, S., New Isotherm for Multilayer Adsorption of Vapours on Non-Porous Adsorbents. *Adsorption Science & Technology* **1985,** 2, (1), 23-30.

22. Vidoni, A.; Ravikovitch, P. I.; Afeworki, M.; Calabro, D.; Deckman, H.; Ruthven, D., Adsorption of CO2 on high silica MFI and DDR zeolites: Structural defects and differences between adsorbent samples. *Microporous and mesoporous materials* **2020,** 294, 109818.

23. Ruthven, D. M.; Kaul, B. K., Adsorption of aromatic hydrocarbons in NaX zeolite. 1. Equilibrium. *Industrial & Engineering Chemistry Research* **1993,** 32, (9), 2047-2052.

24. Sing, K. S. W., Reporting physisorption data for gas/solid systems with special reference to the determination of surface area and porosity (Recommendations 1984). *Pure and Applied Chemistry* **1985,** 57, (4), 603-619.

25. Skarstrom, C. W. Method and apparatus for fractionating gaseous mixtures by adsorption. US Patent 2944627A, 1960.

26. Ruthven, D. M.; Farooq, S.; Knaebel, K. S., *Pressure swing adsorption*. Wiley-VCH, John Wiley & Sons, Inc.: Hoboken, N.J., 1994.

27. Knaebel, K. S.; Hill, F. B., Pressure Swing Adsorption: Development of an Equilibrium Theory for Gas Separations. *Chemical Engineering Science* **1985,** 40, (12), 2351 - 2360.

28. Chiang, A. S. T., An Analytical Solution to Equilibrium PSA Cycles. *Chemical Engineering Science* **1996,** 51, (2), 207 - 216.

29. Owens, D. J.; Ebner, A. D.; Ritter, J. A., Equilibrium Theory Analysis of a Pressure Swing Adsorption Cycle Utilizing a Favorable Langmuir Isotherm: Approach to Periodic Behavior. *Industrial & Engineering Chemistry Research* **2012,** 51, 13454 - 13462.

30. Kayser, J. C.; Knaebel, K. S., Pressure Swing Adsorption: development of an equilibrium

theory for binary gas mixtures with non-linear isotherms. *Chem. Eng. Sci.* **1989,** 44, 1-8.

31. Matz, M. J.; Knaebel, K. S., Pressure Swing Adsorption: Effects of Incomplete Purge. *AIChE Journal* **1988,** 34, (9), 1486 - 1492.

32. Ahn, H., Equilibrium Theory Analysis of Thermal Regeneration of a Humid Adsorption Column: Selection of Optimal Hot Purge Gas Temperature. *Chemical Engineering Research and Design* **2019,** 151, 91 - 99.

33. Rota, R.; Wankat, P. C., Intensification of Pressure Swing Adsorption Processes. *AIChE Journal* **1990,** 36, (9), 1299 - 1312.

34. Luberti, M.; Friedrich, D.; Brandani, S.; Ahn, H., Design of a H2 PSA for Cogeneration of Ultrapure Hydrogen and Power at an Advanced Integrated Gasification Combined Cycle with Pre-combustion Capture. *Adsorption* **2014,** 20, (2-3), 511 - 524.

35. Ahn, H.; Lee, C.-H.; Seo, B.; Yang, J.; Baek, K., Backfill Cycle of a Layered Bed H2 PSA Process. *Adsorption* **1999,** 5, 419 - 433.

36. Ahn, H.; Yang, J.; Lee, C.-H., Effects of Feed Composition of Coke Oven Gas on a Layered Bed H2 PSA Process. *Adsorption* **2001,** 7, 339 - 356.

37. Kayser, J. C.; Knaebel, K. S., Pressure Swing Adsorption: Experimental Study of an Equilibrium Theory. *Chem. Eng. Sci.* **1986,** 41, 2931 - 2938.

TOC graphic

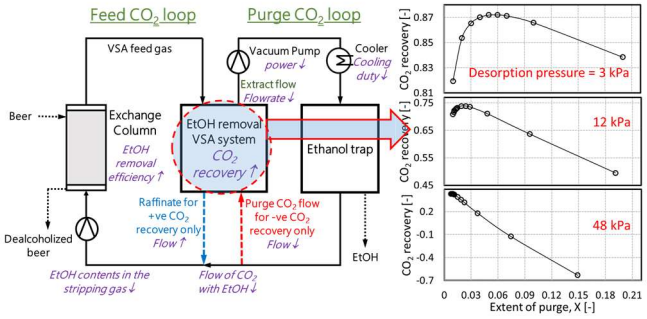
Feed CO_2 loop
Purge CO_2 loop
VSA feed gas
Vacuum Pump
power ↓
Cooler
Cooling duty ↓
Extract flow
Flowrate ↓
Beer
Exchange Column
EtOH removal efficiency ↑
EtOH removal VSA system
CO_2 recovery ↑
Ethanol trap
Raffinate for +ve CO_2 recovery only
Flow ↑
Purge CO_2 flow for -ve CO_2 recovery only
Flow ↓
Dealcoholized beer
EtOH
EtOH contents in the stripping gas ↓
Flow of CO_2 with EtOH ↓
CO_2 recovery [-]
Desorption pressure = 3 kPa
12 kPa
48 kPa
0.87
0.85
0.83
0.81
0.75
0.65
0.55
0.45
0.2
-0.1
-0.4
-0.7
0
0.03
0.06
0.09
0.12
0.15
0.18
0.21
Extent of purge, X [-]